 MCB, vol.4, no.1, pp.27-39, 2007

Theoretical Analysis of Thermal Damage in Biological Tissues Caused by Laser Irradiation

Jianhua Zhou*, J. K. Chen† and Yuwen Zhang‡

Abstract: A bioheat transfer approach is proposed to study thermal damage in biological tissues caused by laser radiation. The laser light propagation in the tissue is first solved by using a robust seven-flux model in cylindrical coordinate system. The resulting spatial distribution of the absorbed laser energy is incorporated into the bioheat transfer equation for solving temperature response. Thermal damage to the tissue is assessed by the extent of denatured protein using a rate process equation. It is found that for the tissue studied, a significant protein denaturation process would take place when temperature exceeds about 53 °C. The effects of laser power, exposure time and beam size as well as the tissue absorption and scattering coefficients on the thermal damage process are examined and discussed. The laser conditions that cause irreversible damage to the tissue are also identified.

Nomenclature

c	specific heat of the tissue, J/(kgK)
c_b	specific heat of blood, J/(kgK)
k	thermal conductivity of tissue, W/(mK)
$L(\overline{r},\hat{s})$	intensity of laser light at position $\overline{r}$ in the $\hat{s}$ direction, W/(m^{2}sr)
$p(\hat{s},\hat{s}')$	phase function of light scattering
q	heat flux, W/m^2
Q_l	internal heat sources due to laser light absorption in the tissue, W/m^3
Q_m	metabolic heat generation, W/m^3
r	coordinate variable in the radial direction, m
r_0	tissue radius, m
r_p	laser beam radius, m
t	time, s
T	temperature, K
T_0	initial temperatue of tissue, K
T_b	blood temperatue, K
w_b	blood perfusion rate, m^3/(m^{3}tissues)
z	coordinate variable in the axial direction, m
z_0	thickness of the tissue, m

Greek symbols

γ	attenuation coefficient, m^{-1}
κ	absorption coefficient, m^{-1}
σ	scattering coefficient, m^{-1}
ρ	mass density of tissue, kg/m^3
ρ_b	mass density of blood, kg/m^3
Ω	damage parameter

1 Introduction

Lasers have been widely used in medical applications for more than three decades. The majority of those applications involve thermal effects. For example, in laser hyperthermia, the temperature of a pathological tissue is often elevated to 42 $\sim$ 45 °C so that the growth of malignant tumor can be retarded. In laser coagulation, laser beams can cause immediate irreversible damage of pathological cells by heating them up to above 60 °C. In laser surgery, a laser beam can vaporize and cut tissues like a scalpel when tissue temperature is heated to as high as 100 °C. No matter which medical treatment is performed, a thorough understanding of the damage distribution within both pathological tissue and the surrounding healthy tissue is imperative.

* Postdoctoral Research Associate. Department of Mechanical and Aerospace Engineering, University of Missouri-Columbia, Columbia, MO 65211

† William & Nancy Thompson Professor. Email: chenjnk@missouri.edu. Department of Mechanical and Aerospace Engineering, University of Missouri-Columbia, Columbia, MO 65211

‡ Associate Professor. Email: zhangyu@missouri.edu. Department of Mechanical and Aerospace Engineering, University of Missouri-Columbia, Columbia, MO 65211

Though experiment is the most realistic means for addressing the medical treatment problems discussed above, it is difficult, if not impossible, to conduct a complete set of experimental tests due to the large variety of tissues, continuing emergence of new lasers, and complexity of the physical and biochemical processes. For that reason, theoretical investigation of thermal damage in laser irradiated tissue has been used as an alternative approach.

Welch [1] described a general, three-step model of laser-tissue interactions, including (1) laser energy deposition in tissue based on the absorption coefficient and scattering coefficient, (2) temperature response modeled by the heat conduction equation, and (3) tissue denaturation evaluated using a rate process equation. Many researchers have followed the Welch's approach by applying different methods to solve the problems involved in the process. For example, Beacco et al. [2] used the beam-broadening method to describe light propagation in tissues and applied the bioheat transfer equation to solve the heat conduction problem. Prahl et al. [3] presented a thermal damage model for laser welding process. They adopted the Beer's law for volumetric laser heat source and the rate process equation for thermal damage. In the heat conduction analysis, a lump heat capacity approach was employed before tissue was vaporized and a one-dimensional (1-D) analytical solution after the evaporation. Recently, Zhu et al. [4] utilized the diffusion theory to evaluate light energy deposition in the tissue, along with the bioheat equation for the heat transfer and the rate process model for the resulting thermal damage. Diaz et al. [5, 6] developed a thermal damage model for the laser irradiated cartilage, in which the heat diffusion equation in the tissue slab was solved using a finite element method.

The most distinction among the theoretical approaches mentioned above is the description of the spatial distribution of laser energy absorbed by tissue, which is crucial in determination of thermal response and the subsequent tissue damage. In addition, little work has been done to examine the effects of laser parameters and tissue optical properties to date. In this study, the bioheat transfer equation together with a robust seven-flux light propagation model for laser energy deposition and the rate process model for tissue damage is proposed to investigate irreversible thermal damage in biological soft tissues. The effects of laser parameters and tissue optical properties on thermal damage in the irradiated tissues are examined and discussed.

2 Mathematical Model

Consider a tissue irradiated by a continuous wave laser beam with a constant power for a period of time t_p. The beam has a Gaussian spatial profile of radius r_p, defined as the radial distance at the $1/e^2$ points of the pulse intensity distribution. It is applied normally to the upper surface of the tissue. Let the center of the incident laser beam coincide with the origin of a cylindrical coordinate system (Fig. 1). The tissue is initially at uniform temperature T_0, and the other boundary surfaces are thermally insulated to the environments. Assume that the tissue is an isotropic material. Due to symmetry, a 2-D axisymmetric model is depicted in Fig. 1 for the tissue with a radius of r_0 ($r_0 \geq r_p$) and a thickness of z_0.

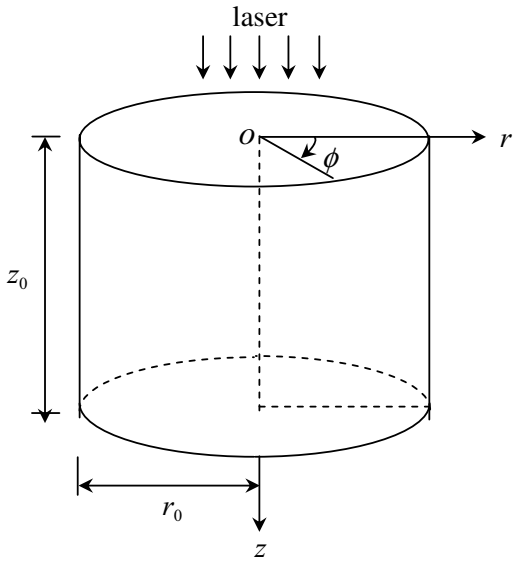

Figure 1: A schematic of physical model

2.1 Axisymmetric Bioheat Transfer Equation

Heat transfer in a mammaliam tissue is quite complicated due to the geometry of micro blood vessels. To keep the problem tractable and mathematically feasible, the tissue is frequently assumed to be macroscopically homogeneous and isotropic. The most commonly used equation for heat transport in the tissue is the Pennes' bioheat equation [7], which includes blood flow and metabolism to the classical Fourier's heat conduction equation

$$\rho c\frac{\partial T}{\partial t} = \nabla\cdot(k\nabla T) + \rho_b c_b w_b(T_b - T) + Q_m \quad (1)$$

where ρ is tissue mass density; ρ_b is blood mass density; c is specific heat of the tissue; c_b is specific heat of blood; T and T_b are the temperatures of tissue and blood, respectively; k is thermal conductivity of tissue; w_b is the blood perfusion rate; Q_m is the metabolic heat generation.

For a biological soft tissue irradiated by a laser beam described previously, the axisymmetric bioheat transfer equation is written as:

$$\rho c\frac{\partial T}{\partial t} = \frac{1}{r}\frac{\partial}{\partial r}\left(kr\frac{\partial T}{\partial r}\right) + \frac{\partial}{\partial z}\left(k\frac{\partial T}{\partial z}\right) + \rho_b c_b w_b(T_b - T) + Q_m + Q_l \quad (2)$$

where Q_l is the volumetric laser heat source. In this study, Eq. (2) is solved with the following initial and boundary conditions:

$$T(r,z;0) = T_0, \quad q_r(r,z;0) = 0, \quad q_z(r,z;0) = 0 \quad (3)$$

$$q_r(0,z;t) = q_r(r_0,z;t) = 0 \quad (4)$$

$$q_z(r,0;t) = q_z(r,z_0;t) = 0 \quad (5)$$

2.2 Light propagation

Light propagation in soft bio-tissues is much more complicated than industry solids due to the non-homogeneous tissue structures and anisotropic scattering. Though the Beer's law can be used to approximate the spatial distribution of absorbed laser energy in the tissue by combining optical penetration depth and the light scattering depth as did in Reference [3], a more reliable description is needed to solve the collimated and scattering light propagation in the medium. The laser light propagation in a biological tissue is described by the equation of radiation transfer [8-12]:

$$\hat{s}\cdot\nabla L(\overline{r},\hat{s}) + \gamma L(\overline{r},\hat{s}) = \frac{\gamma}{4\pi}\int_{4\pi} p(\hat{s},\hat{s}')L(\overline{r},\hat{s}')d\omega' \quad (6)$$

where $\overline{r}$ is a position vector, $\hat{s}$ and $\hat{s}'$ are the direction vectors, $L(\overline{r},\hat{s})$ is the intensity of laser light at position $\overline{r}$ in the $\hat{s}$ direction, ω' is the solid angle, and $p(\hat{s},\hat{s}')$ is the phase function representing the scattering contribution from $\hat{s}'$ to the $\hat{s}$ direction. The unit of L in Eq. (6) is W/(m^{2}sr). The solid angle integration of the phase function is given by

$$\frac{1}{4\pi}\int_{4\pi} p(\hat{s},\hat{s}')d\omega' = \frac{\sigma}{\gamma} \quad (7)$$

where γ is the attenuation coefficient defined as the sum of the absorption coefficient (κ) and the scattering coefficient σ.

An exact analytical solution of Eq. (6) for $L(\overline{r},\hat{s})$ is impossible for multi-dimensional geometries. Although the Kubelka-Munk's approach [13] is a useful tool for solving Eq. (6), it is restricted to 1-D geometries. Diffusion theory [14] provides a fast approach to approximating some physical quantities of light transport in turbid media, but they are invalid near the photon source or the boundary where the laser intensity is strongly anisotropic. Monte Carlo simulation [15-17] offers a flexible and accurate approach toward photon transport in turbid media; however, it is computational intensive. Yoon et al. [18] proposed a seven-flux model in Cartesian coordinates to compute light distribution in laser-irradiated tissue. In the seven flux model, the differential-integral equation is converted to a linear system of equations and thus a fast and accurate algorithm can be achieved.

Recently, Zhou et al. [19] reformulated the seven-flux model in cylindrical coordinates. The laser light scattering in tissue is described by a simple pattern of seven weighted directional fluxes. The governing equations for the seven components of light fluxes in a cylindrical coordinate system (r,z,ϕ), depicted in Fig. 1, are expressed

as follows:

$$\frac{\partial F_c(r,z,\phi)}{\partial z} = -\gamma F_c(r,z,\phi) \tag{8}$$

$$\frac{\partial F_{x_i}(r,z,\phi)}{h\partial x_i} + \gamma F_{x_i} = \gamma\Big[p_{x_i,+r}F_{+r} + p_{x_i,-r}F_{-r} + p_{x_i,+\phi}F_{+\phi} + p_{x_i,-\phi}F_{-\phi} + p_{x_i,+z}F_{+z} + p_{x_i,-z}F_{-z} + p_{x_i,+z}F_c\Big] \quad (x_i = \pm r, \pm z, \pm\phi) \tag{9}$$

where F_c is the collimated light flux in the $+z$ direction; $F_{\pm r}$, $F_{\pm z}$ and $F_{\pm\phi}$ are the six components of the scattered light flux in the $\pm r$, $\pm z$ and $\pm\phi$ directions, respectively; $h = 1,1,r$ for $x_i = \pm r, \pm z, \pm\phi$, respectively; p_{ij} is the portion of flux scattered from the j-direction into the i-direction, representing the phase function $p(\hat{s},\hat{s}')$ in Eq. (6). Detailed calculation of p_{ij} can be found in References [18, 19]. Because of the axisymmetric nature considered here, $F_\phi = F_{-\phi}$. The number of the governing equations (9) thus reduce to 5.

Once the values of all the seven discrete fluxes components are determined, laser intensity $L(\overline{r},\hat{s})$ (W/m^2-sr) can be reconstructed by using the relations between the discrete fluxes and the intensity. The collimated flux F_c is related to the collimated intensity $L_c(\overline{r},\hat{s})$ as:

$$F_c(\overline{r}) = \frac{L_c(\overline{r},\hat{s})}{\delta(\cos\theta - 1)\delta(\varphi)} \tag{10}$$

where the direction vector $\hat{s}$ is expressed as the directional angles θ and ϕ, and δ is the delta function. The solution of the collimated intensity L_c in Eq. (10) is straightforward. The relations between the scattered flux components $F_{\hat{s}}$ and the scattered intensity $L_s(\overline{r},\hat{s})$ are

$$F_{\hat{s}}(\overline{r}) = \int_{2\pi,\hat{s}} L_s(\overline{r},\hat{s}')(\hat{s}\cdot\hat{s}')d\omega' \tag{11}$$

where $\hat{s} = \pm r, \pm z, \pm\phi$. Though the scattered intensity L_s is implicitly included in Eq. (11), it can be solved by expanding the intensity L_s into the associated Legendre polynomials. With the Legendre polynomial expansion of L_s in Eq. (11), a linear system of equations is formed in which the unknown coefficients in the Legendre polynomial expansions can be easily solved.

The rate of volumetric heat generation $Q_l(\overline{r})$ due to the absorption of light in tissue is proportional to the fluence rate and the absorption coefficient as follows:

$$Q_l(\overline{r}) = \kappa\int_{4\pi} L(\overline{r},\hat{s})d\omega = \kappa\int_{4\pi}[L_c(\overline{r},\hat{s}) + L_s(\overline{r},\hat{s})]d\omega \tag{12}$$

In the present study, the above seven-flux scheme in the cylindrical coordinate is employed to simulate laser light propagation in tissue. The resulting spatial distribution of the absorbed laser energy is the volumetric heat source Q_l in the bioheat conduction equation (2).

2.3 Damage Prediction

To quantify the extent of thermal damage in a living tissue, a damage parameter Ω is defined as [1]:

$$\Omega = \ln\left(\frac{C_0}{C_0 - C_d}\right) \tag{13}$$

where C_0 is the protein concentration in non-irradiated tissue, and C_d is the concentration of denaturated protein. The tissue is assumed to be irreversible damage when $\Omega \geq 1.0$ [1], which corresponds to a threshold denaturation of 63% of the molecules.

The protein denaturation process is considered as a chemical reaction. The damage parameter Ω can be evaluated according to the Arrenius equation:

$$\Omega(r,z,t) = A\int_{t_1}^{t_f}\exp\left(-\frac{E}{RT}\right)dt \tag{14}$$

where A is the frequency factor; E is the energy of activation of denaturation reaction; R is the universal gas constant, 8.314 J/(molK); T is the absolute temperature of the tissue at the point where Ω is calculated; t_1 is the time at the onset of laser exposure; t_f is the time when the thermal damage is evaluated. Numerical values for the frequency factor and the activation energy are given as: $A = 3.1\times10^{98}$ s^{-1}; $E = 6.28\times10^5$ J/mol [1].

3 Results and Discussion

A 2-D axisymmetric finite difference code is developed by incorporating the seven-flux model into the bioheat conduction equation. The physical properties of the biological tissue used in the numerical analysis are [20]: ρ = 1000 kg/m^3, k= 0.628 W/(mK), c= 4187 J/(kgK), ρ_b = 1.06×10^3 kg/m^3, c_b= 3860 J/(kgK), w_b= 1.87×10^{-3} m^3/(m^{3}tissues), $T_b = 37°$, and Q_m= 1.19×10^3 W/m^3. The tissue optical properties are [2]: $\sigma = 10.6\ \text{cm}^{-1}$, and $\kappa = 0.4\ \text{cm}^{-1}$. The radius and thickness of the cylindrical tissue are 5 mm, respectively. The initial temperature T_0 of the tissue is 37 °C. Convergence study on the grid size and time increment is first carried out. It is found that a mesh of 100×100 points and a time step of 0.01s are adequate and used in the following simulations.

Figure 2 shows the evolutions of temperature T and the damage parameter Ω calculated at the center $(0,0,0)$ of the heated surface. In this simulation, the laser power is 5 W, beam radius (r_p) is 2 mm, and exposure time is 2.3 s. As expected, the temperature increases with time, reaches a maximum value at the time when laser is turned off, and then falls down due to heat diffusion into the surrounding bulk. It is seen from Fig. 2 that the damage parameter is rather low until temperature rises to about 53 °C. Afterward, the value of the damage parameter rises very fast, continues to increase even after the laser is turned off, and then becomes saturated when the temperature cools down to about 53 °C. The different time histories of the temperature and of the damage parameter indicate that one cannot obtain true information about the thermal damage in an irradiated tissue simply according to the transient temperature response. In fact, the result in Fig. 2 shows that the protein denaturation process always takes place as long as the tissue temperature exceeds about 53 °C.

In the following, the effects of laser exposure time, power and beam size as well as the light absorption and scattering in tissues are examined. All the laser and material properties given above are employed except for the parameter or property whose effect is examined.

3.1 Laser Exposure Time

Figure 3 shows the effect of laser exposure time on the temperature and damage parameter at the center of the heated spot. For comparison, three consecutive exposure times (2.3 s, 2.4 s and 2.5 s) are considered. As shown in Fig. 3, the starting time of steep rise of the damage parameter does not influenced by the exposure time. However, the longer the exposure time is, the more time is required for the damage parameter to reach its steady value. This can be explained with the finding in Fig. 2 that the protein denaturation occurs when temperature is greater than about 53 °C. The results shown in Fig. 3 reveals that for the laser power of 5 W, the tissue would be irreversibly damaged ($\Omega \geq 1.0$) when the exposure time is in between 2.4 s and 2.5 s.

3.2 Laser Power

Figure 4 shows the effect of laser power on the temperature and damage parameter at the central point $(0,0,0)$. It appears, as expected, that the higher the laser power, the earlier and steeper the damage parameter and the greater the saturated damage parameter. The reason is that temperature would rise faster and higher when laser power is higher. The faster temperature rise makes the onset time of the protein denaturation earlier; the higher temperature prolongs the protein denaturation process because it takes a longer time for tissue to cool down below 53 °C. For the laser exposure time of 2.3 s, the power needed to cause the tissue irreversible damage is in between 5.0 W and 5.5 W.

3.3 Laser Beam Size

Figure 5 shows the effect of laser beam size on the temperature and damage parameter at the center of the heated area. The trends of the results in Fig. 5 are opposite to those in Fig. 4. The smaller the beam size is, the earlier and steeper the damage parameter would rise and the greater the damage parameter saturates. The radius of the laser beam that causes the tissue irreversible damage is

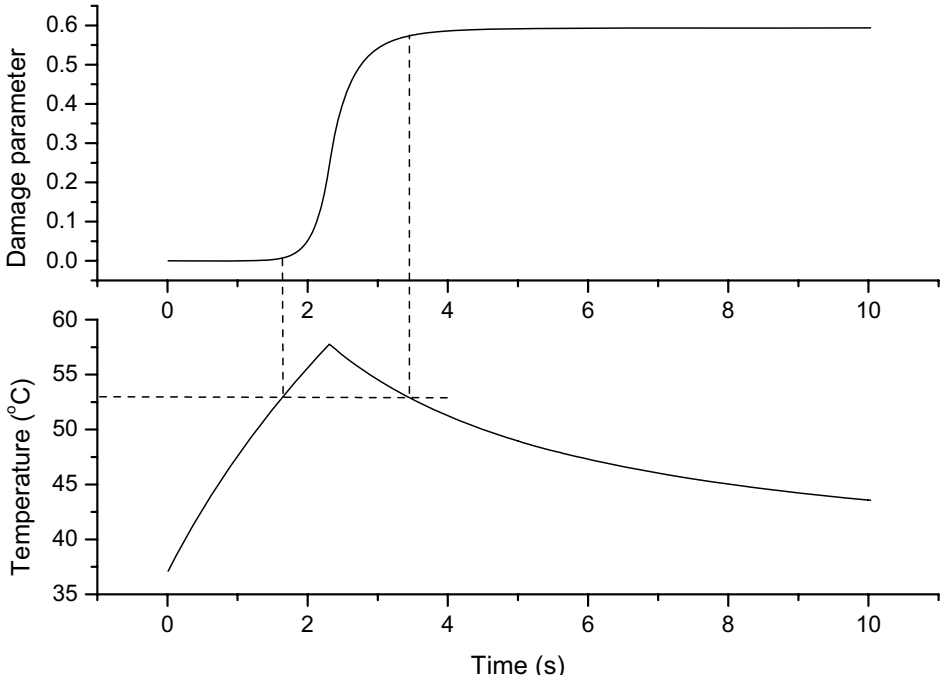

Figure 2: Temperature and damage parameter at the center $(0,0,0)$ of the heated area as a function of time

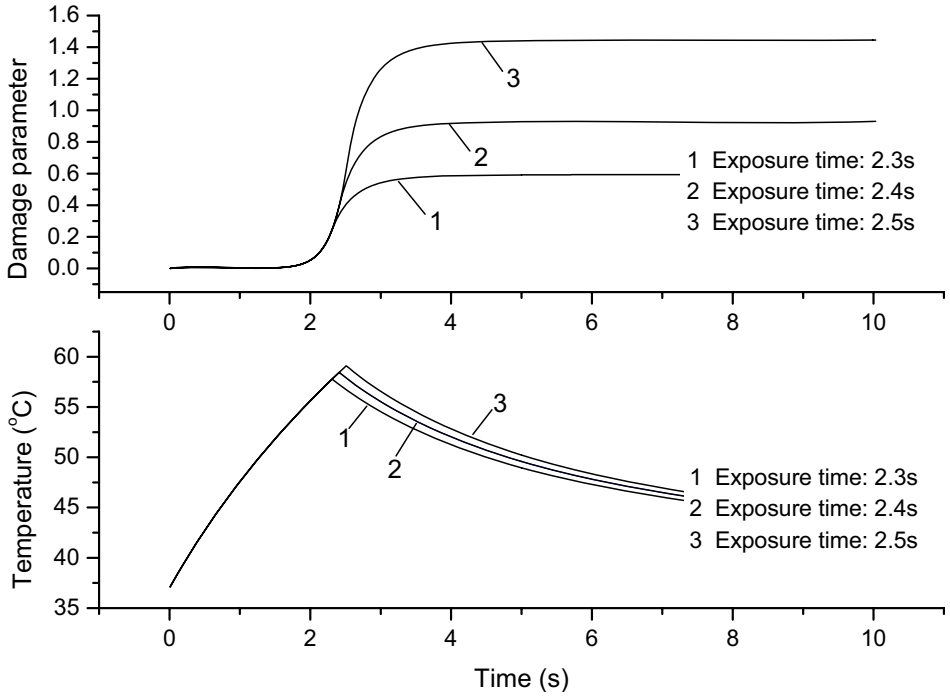

Figure 3: Effect of exposure time on temperature and damage parameter at the center of the heated area

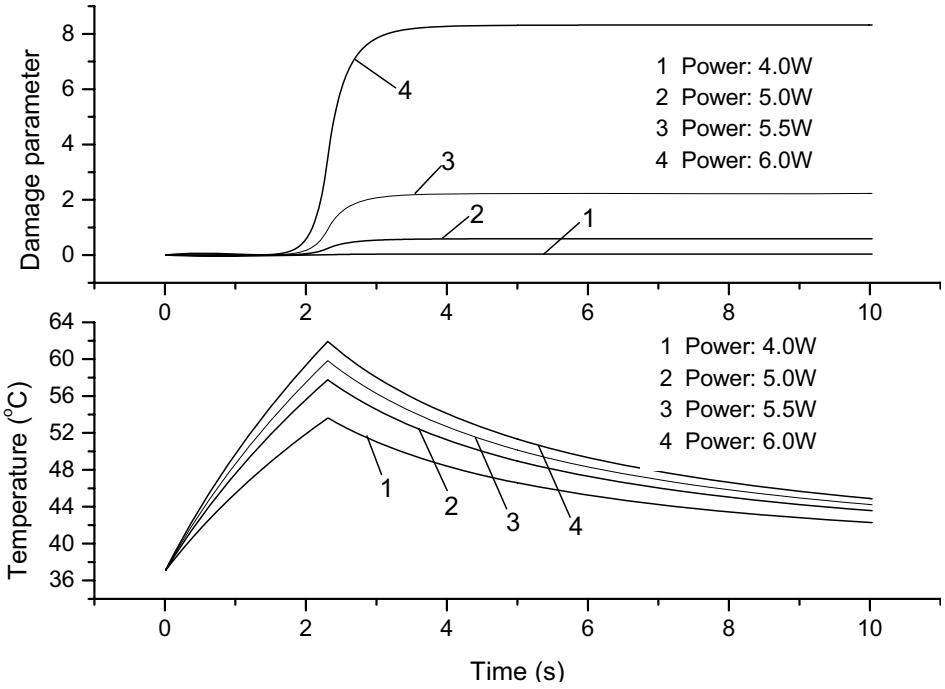

Figure 4: Effect of laser power on temperature and damage parameter at the center of heated area

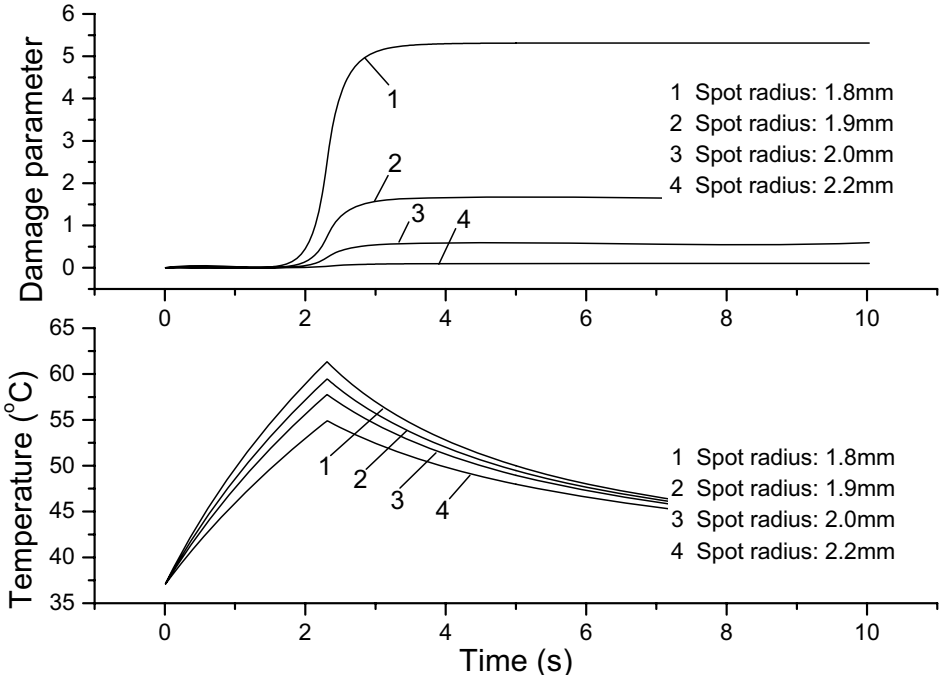

Figure 5: Effect of spot radius on temperature and damage parameter at the center of heated area

in between 1.9 mm and 2.0 mm for the power of 5.0 W and duration of 2.3 s.

The 2-D distributions of the saturated damage parameter are displayed in Fig. 6 for two laser beams of r_p = 1.8 mm and 2.0 mm. It is obvious that a laser beam with a smaller radius not only results in more serious damage but also leads to a larger damage size.

As the foregoing examinations, a more serious damage to tissue can be caused by a laser beam either having a higher power or having a smaller beam size. This is attributed to the fact that laser intensity increases with increasing of the power or decreasing of the beam size. A general conclusion can thus be made that the higher the laser intensity, the more severe the thermal damage.

Figure 7 shows the thermal diffusion effect on the temperature and damage parameter at the center of the heated spot. To keep the laser intensities identical, different power and beam radius are chosen for the two cases shown in the figure. Apparently, the case of the laser power 6.05 W and radius r_p = 2.2 mm almost doubles the value of the damage parameter and leads to an irreversible damage to the tissue. The only difference of the thermal response between these two cases is heat diffusion. It would take a longer time for a larger heating area to diffuse its thermal energy to the surrounding bulk than for a smaller one. As a result of the greater temperature induced and the longer time required for cooling down for the region in the central part of the heated area, the resulting damage would be more severe.

3.4 Scattering Coefficient

The optical properties could vary significantly from one tissue to another, thereby resulting in different temperature field and consequently different thermal damage. Figure 8 shows the effect of tissue scattering coefficient on the temperature and damage parameter at the center of the heated area. As shown in the figure, both the temperature and damage parameter increase as the scattering coefficient increases. This means that a larger scattering coefficient could lead to a more serious damage. Figure 8 also indicates that the increase in temperature and the damage parameter becomes slowly when the scattering coefficient further increases.

The 2-D distributions of the saturated damage parameter are plotted in Fig. 9 for two scattering coefficients $\sigma = 5\,\mathrm{cm}^{-1}$ and $10.6\,\mathrm{cm}^{-1}$. As shown in Fig. 9, the damage parameter tends to increase in both the axial and radial directions when the tissue scattering coefficient is higher. This is because laser intensity is proportional to the exponential function $\exp(-\sigma z)$, implying that more laser energy is absorbed in the region near the irradiated surface for tissues having a larger scattering coefficient. Consequently, the resulting temperature is higher and the thermal damage in this region is more severe.

3.5 Absorption Coefficient

Figures 10 and 11 illustrate the effect of tissue absorption coefficient on the temperature and damage parameter. The general effects are similar to those of the scattering coefficient. The higher the absorption coefficient, the earlier and steeper the damage parameter rise and the greater the saturated damage parameter. Comparing the results in Figs. 8-11 shows that the effect of the absorption coefficient is more significant than that of the scattering coefficient.

4 Conclusions

This paper presents a three-step model to investigate thermal damage in laser irradiated biological tissues. The seven-flux model in cylindrical coordinates is employed to calculate the light propagation; the temperature distribution in the tissue is predicted by the bioheat transfer equation; the thermal damage is estimated by the rate process model. The effects of laser irradiation parameters and the optical properties of tissue on the thermal damage are examined. For the tissue cases studied in this work, it is found that protein denaturation would take place significantly when temperature in the tissue exceeds about 53 °C. When a tissue is irradiated by a continuous wave laser beam having a constant power in time, the damage parameter would still accumulates even after laser is turned off. Therefore, the most serious

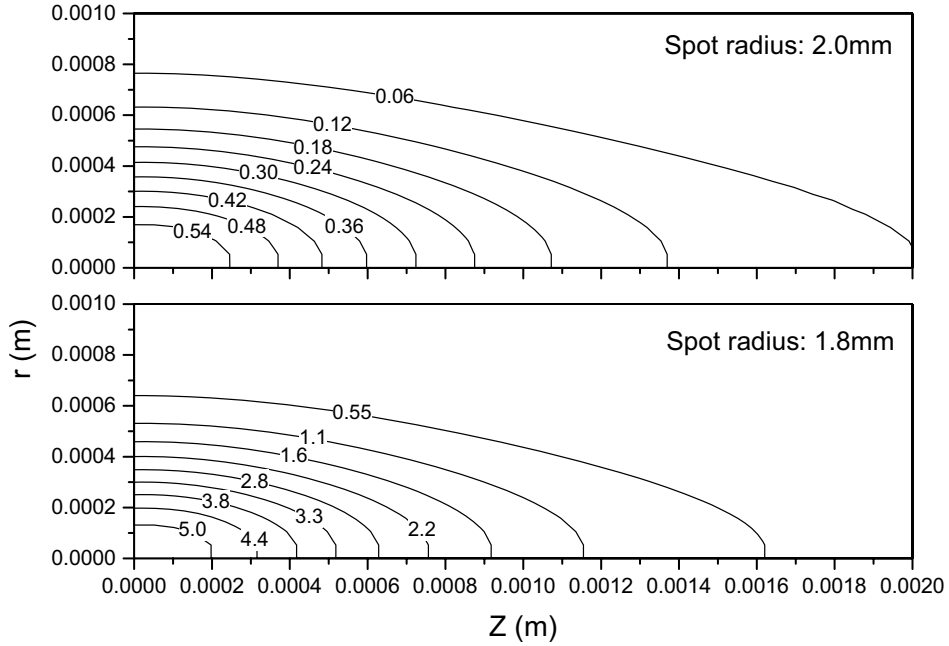

Figure 6: Two-dimensional distribution of the damage parameter for beam radius of r_p = 1.8 mm and 2.0 mm

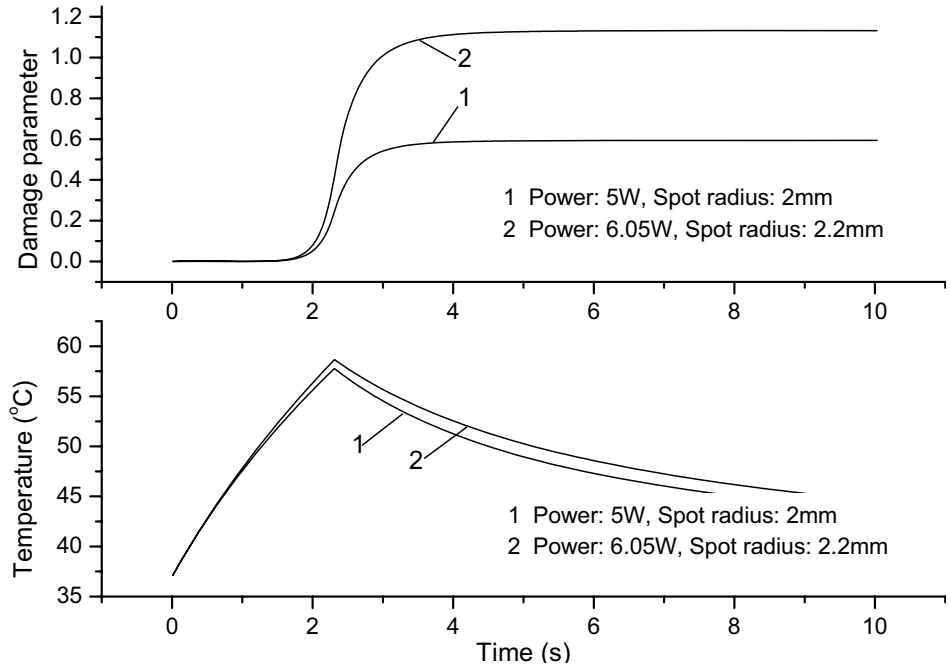

Figure 7: Effect of power density on temperature and damage parameter at the center of heated area

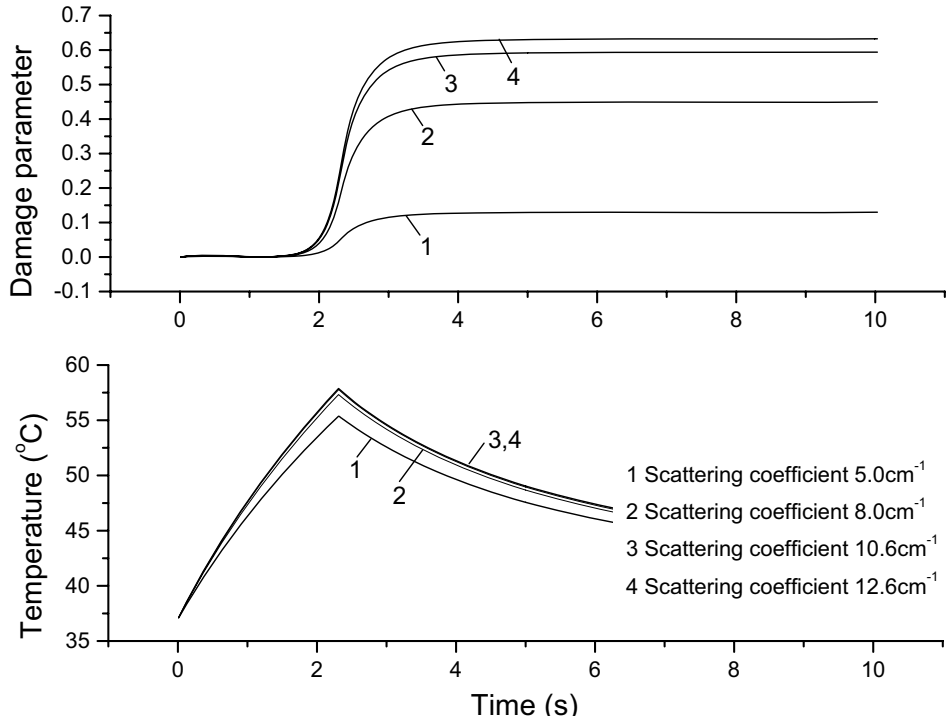

Figure 8: Effect of scattering coefficient on temperature and damage parameter at the center of heated area

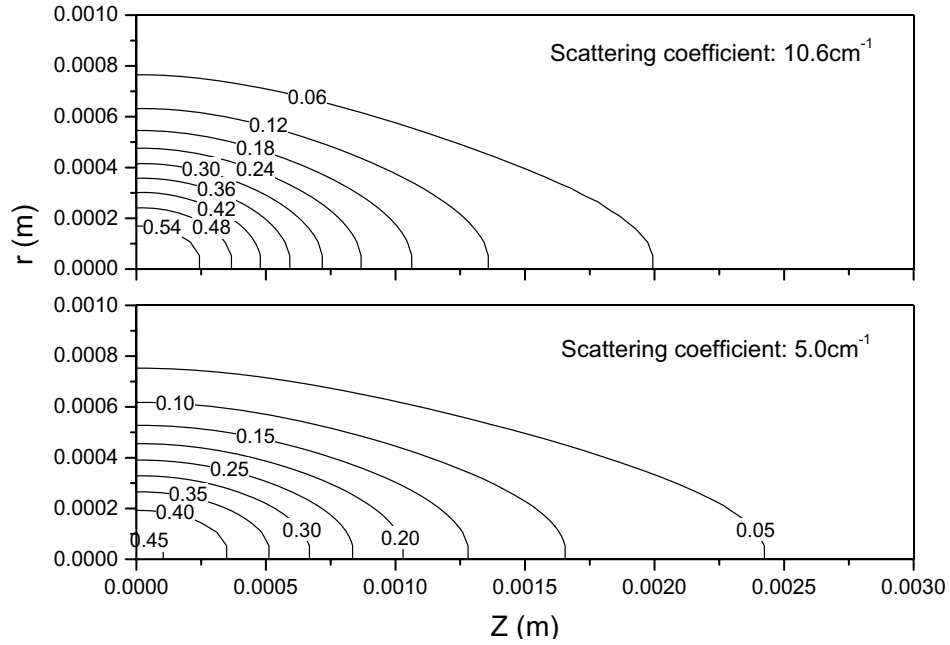

Figure 9: Two-dimensional distribution of damage parameter for σ = 5 cm^{-1} and 10.6 cm^{-1}

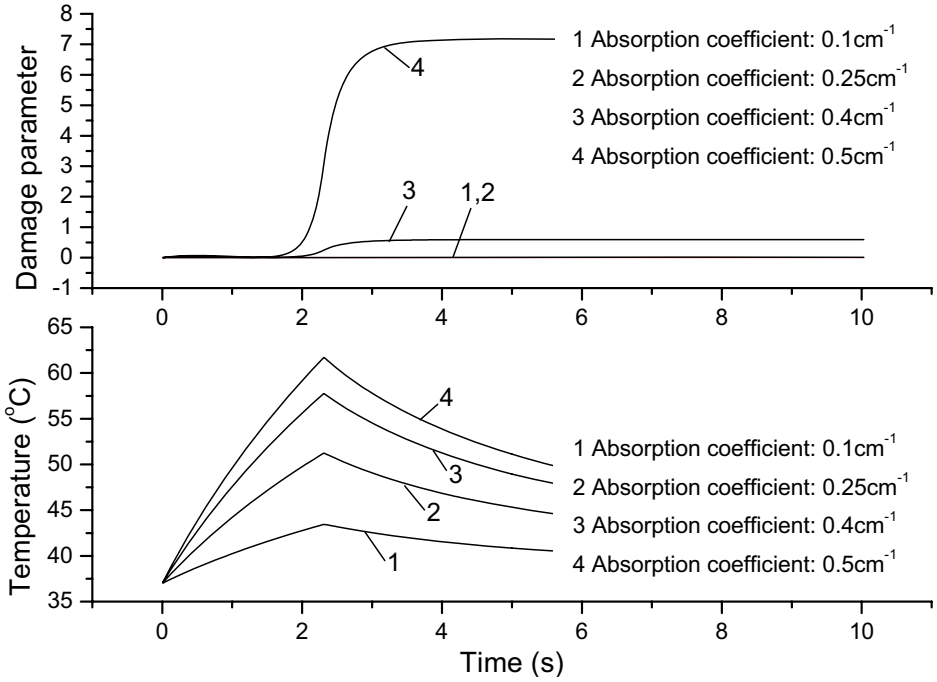

Figure 10: Effect of absorption coefficient on temperature and damage parameter at the center of heated area

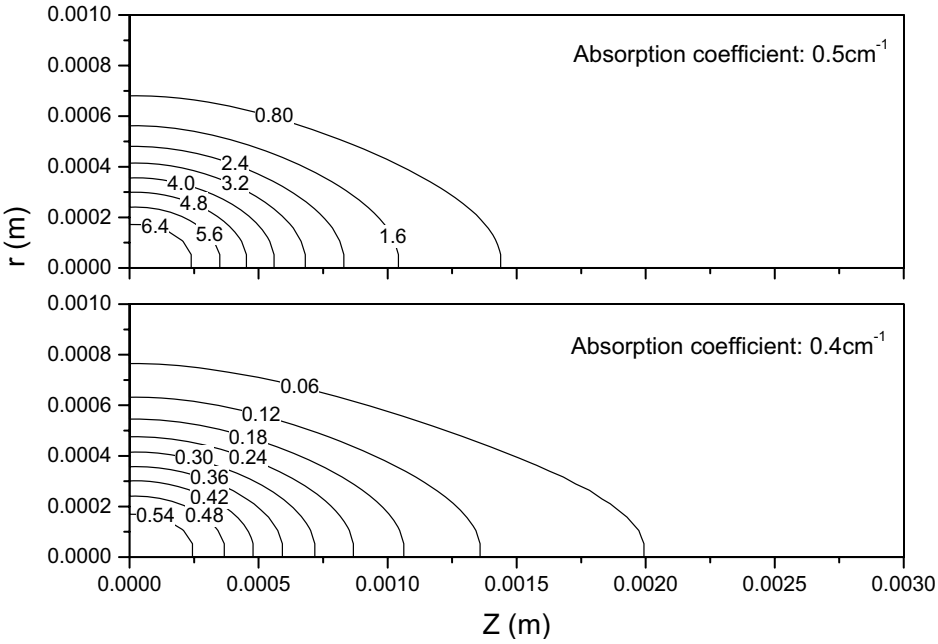

Figure 11: Two-dimensional distribution of damage parameter for $\kappa = 0.4$ cm^{-1} and 0.5cm^{-1}

tissue damage occurs sometime after the laser irradiation, i.e., when the temperature cools down to about 53 °C. It is also shown that lasers having a higher intensity, longer exposure time, or wider beam size would cause more severe thermal damage to tissue than its counterpart beam. The general trends of the effect of tissue scattering and absorption coefficients on the thermal damage are similar. The higher the absorption (or scattering) coefficient, the more serious and the lager size the damage. However, the effect of the absorption coefficient is more significant than that of the scattering coefficient.

References

1. **Welch, A. J.** (1984): The thermal response of laser irradiated tissue, *IEEE Journal of Quantum Electronics*, **20**(12), pp. 1471-1481.

2. **Beacco, C. M.; Mordon, S. R.; Brunetaud, J. M.** (1994): Development and experimental in vivo validation of mathematical modeling of laser coagulation, *Lasers in Surgery and Medicine*, **14**, pp. 362-373.

3. **Prahl, S. A.; Pearson, S. D.** (1997): Rate process models for thermal welding, *Laser-Tissue Interaction VIII*, Jacques, S. L., Ed., *Proceedings of the SPIE*, **2975**, pp. 245-252.

4. **Zhu, D.; Luo, Q. M.; Zhu, G. M.** (2002): Kinetic thermal response and damage in laser coagulation of tissue, *Lasers in Surgery and Medicine*, **31**(5), pp. 313-321.

5. **Diaz, S. H.; Lavernia, E. J.; Wong, B. J. F.** (2001): Modeling the thermal response of porcine cartilage during laser irradiation, *IEEE Journal of Selected Topics in Quantum Electronics*, **7**(6), pp. 944-951.

6. **Diaz, S. H.; Nelson, J. S.; Wong, B. J. F.** (2003): Rate process analysis of thermal damage in cartilage, *Physics in Medicine and Biology*, **48**, pp. 19-29.

7. **Pennes, H. H.** (1948): Analysis of tissue and arterial blood temperatures in the resting forearm, *Journal of Applied Physiology*, **1**, pp. 93-122.

8. **Ishimaru, A.** (1978): *Wave Propagation and Scattering in Random Media*, Academic Press, New York.

9. **Siegel, R.; Howell, J. R.** (1992): *Thermal Radiation Heat Transfer*, 3rd Edition, Hemisphere, Washington, DC.

10. **Welch, A. J.; van Gemert, M. J. C.** (1995): *Optical-Thermal Response of Laser-Irradiated Tissue*, Plenum Press, New York.

11. **Niemz, M. H.** (2002):, *Laser-Tissue Interactions: Fundamentals and Applications*, Springer-Verlag, Berlin.

12. **Modest, M. F.** (2003): *Radiative Heat Transfer*, 2nd Edition, Academic Press, New York.

13. **Egan, W. G.; Hilgeman, T. W.** (1979): *Optical Properties of Inhomogeneous Materials—Applications to Geology, Astronomy, Chemistry and Engineering*, Academic Press, New York.

14. **Farrell, T. J.; Patterson, M. S.; Wilson, B. C.** (1992): A diffusion theory model of spatially resolved, steady-state diffuse reflectance for the non-invasive determination of tissue optical properties in vivo, *Medical Physics*, **19**, pp. 879-888.

15. **Wilson, B. C.** (1983): A Monte Carlo model of the absorption and flux distributions of light in tissue, *Medical Physics*, **10**(6), pp. 824-830.

16. **Hasegawa, Y.; Yamada, Y.; Tamura, M.; Nomura, Y.** (1992): Monte Carlo simulation of light transimission through living tissues, *Applied Optics*, **30**(31), pp. 4515-4520.

17. **Wang, L.; Jacques, S. L.; Zheng, L.** (1995): MCML–Monte Carlo modeling of light transport in multi-layered tissues, *Computer Methods and Programs in Biomedicine*, **47**, pp. 131-146.

18. **Yoon, G.; Welch, A. J.; Motamedi, M.; van Gemert, M. C. J.** (1987): Development and application of three-dimensional light distribution model for laser irradiated tissue, *IEEE Journal of Quantum Electronics*, **23**(10), pp. 1721-1732.

19. **Zhou, J.; Liu, D.; Xu, J.; Huai, X.** (2002): Seven-flux modeling of laser light propagation in biological tissue in cylindrical coordinates, *Acta Photonica Sinica*, **31**(6), pp. 662-667, 2002 (in Chinese).

20. **Yamada, Y.; Tien, T.; Ohta, M.** (1995): Theoretical analysis of temperature variation of biological tissues irradiated by light, *ASME/JSME Thermal Engineering Conference*, **4**, pp. 575-581.